PCCP

PAPER

View Article Online
View Journal | View Issue

Cite this: *Phys. Chem. Chem. Phys.*, 2015, **17**, 19350

Cyclic voltammetry of fast conducting electrocatalytic films†

Cyrille Costentin* and Jean-Michel Savéant*

Received 15th May 2015,
Accepted 25th June 2015

DOI: 10.1039/c5cp02825f

www.rsc.org/pccp

In the framework of contemporary energy challenges, cyclic voltammetry is a particularly useful tool for deciphering the kinetics of catalytic films. The case of fast conducting films is analyzed, whether conduction is of the ohmic type or proceeds through rapid electron hopping. The rate-limiting factors are then the diffusion of the substrate in solution and through the film as well as the catalytic reaction itself. The dimensionless combination of the characteristics of these factors allows reducing the number of actual parameters to a maximum of two. The kinetics of the system may then be fully analyzed with the help of a kinetic zone diagram. Observing the variations of the current–potential responses with operational parameters such as film thickness, the potential scan rate and substrate concentration allows a precise assessment of the interplay between these factors and of the values of the rate controlling factors. A series of thought experiments is described in order to render the kinetic analysis more palpable.

Introduction

In the framework of contemporary energy challenges, the increasing importance of devices based on the coating of electrodes by electrocatalytic films[1–8] calls for the development of reliable techniques for analyzing the functioning of these films. Cyclic voltammetry (CV) appears to be a particularly valuable technique for this purpose, having the advantage over steady-state techniques, such as rotating disk electrode voltammetry (RDEV), of simplicity and rapidity of the current–potential curve recording and the larger extent by which the rate of substrate diffusion may be varied through the rate of potential scanning as compared to the rotation rate in RDEV.

In a previous article,[9] we have laid the fundamental bases of the application of cyclic voltammetry to the kinetic analysis of catalytic films with the aim of deciphering the interplay between the rate controlling factors inside and outside the film. A first illustration of this approach was then given in the simple case where the substrate concentration is practically constant in the film and in the solution. This situation involves the important cases where the substrate is the solvent as in the catalysis of water oxidation or reduction. A series of thought experiments was then described to illustrate more tangibly the strategies to be applied for characterizing the functioning of the catalytic film under these conditions.

Université Paris Diderot, Sorbonne Paris Cité, Laboratoire d'Electrochimie Moléculaire, Unité Mixte de Recherche Université – CNRS No. 7591, Bâtiment Lavoisier, 15 rue Jean de Baïf, 75205 Paris Cedex 13, France. E-mail: cyrille.costentin@univ-paris-diderot.fr, saveant@univ-paris-diderot.fr

† Electronic supplementary information (ESI) available: Derivation of the equations of Chart 1. Numerical resolution of the integral-equation expressions. See DOI: 10.1039/c5cp02825f

We now address the case of fast conducting films. It includes the case where charge transport proceeds through rapid electron hopping. It is also relevant to the numerous and important systems where conduction is ohmic as when various sorts of carbon additives are mixed with the catalyst.[10–16] In this framework, we expect the kinetic behavior of the film to be jointly governed by the catalytic reaction and the substrate diffusion inside the film as represented in Fig. 1. The catalytic reaction may be second order, with explicit dependence upon substrate concentration or pseudo-first order as when the substrate is the solvent. The role of substrate diffusion from the bulk of the solution to the solution/film interface will have also to be taken into account. This amounts to a transposition to cyclic voltammetry of the Koutecky–Levich approach of rotating disk electrode voltammetric experiments.[17,18]

Here too we report a series of thought experiments designed to make more palpable the kinetic analyses of such systems.

Results and discussion

Kinetic zone diagram and expression of the current–potential curves

The phenomena that govern the kinetics – diffusion of substrate in the solution toward the film-solution interface, substrate permeation through the film and catalytic reaction associated as shown in Fig. 1 – are represented by characteristic current densities. Their definitions, involving diffusion coefficients, catalyst and substrate concentrations, film thickness, and rate constant are recalled in the Symbols and definitions section together with the definition of symbols used. We note that the

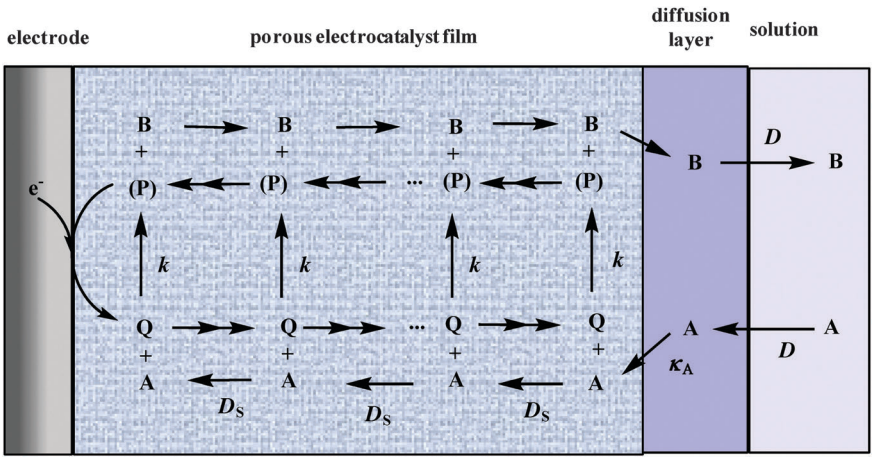

Fig. 1 Schematic representation of the porous electrocatalytic film, of the catalytic reaction and of the mass (diffusion) and charge transport (fast electron hopping or ohmic conduction) processes. The scheme is for reductions. Transposition to oxidation is straightforward. The symbols in the scheme are self-explaining. Their definitions are recalled in the list of symbols.

current density characterizing the charge transport through the film that was involved in the previous general analysis[9] is no longer required since charge transport is assumed to be fast whether it involves electron hopping or ohmic conduction.

We also assume that the catalytic reaction is fast enough for pure kinetic conditions to be achieved.[19] A steady state is thus established for the concentrations of Q and A as the result of mutual compensation between catalytic reaction and diffusion. This results, at the mathematical level, in the absence of time variation of the concentrations of Q and A:

$$\frac{\partial C_A}{\partial t} \approx 0 = D_S \frac{\partial^2 C_A}{\partial x^2} - kC_A C_Q$$

This is not a very stringent condition in practice since the most interesting catalytic systems are those in which the catalytic reaction itself is fast.

The cyclic voltammetric current–potential response of the system is expressed in a dimensionless way as the ratio I/I_A between the observed current density and the current density representing the substrate diffusion in solution, referred to a dimensionless potential scale – $-(F/RT)(E - E^0)$ – centered on the catalyst standard potential, E^0. It depends in the general case of two dimensionless parameters that may be chosen as I_A/I_S and I_S/I_k or of any two linear combinations of these two parameters. The dimensionless expression of the current–potential response in this case is given in the center of Chart 1. The acronym chosen for designating this situation, R + S, indicates that the overall reaction is governed jointly by the catalytic reaction (R) and diffusion of the substrate in the film (S).[17]

Starting from the general case and going to extreme (0 or ∞) values of the dimensionless parameters, the dimensionless formulations of the CV responses simplify to expressions that depend on a single parameter and then on no parameter at all. In the latter case, this does not mean that the experimental CV trace does not depend on any experimental parameter but rather that the effect of varying the experimental parameters is contained in the very dimensionless expression of the CV response as given in Chart 1.

The effect of varying the parameters is better represented by a zone diagram such as the one shown in Fig. 2, the axes of which are the same two dimensionless parameters as introduced earlier. Then, travelling through the diagram along one of these coordinates or along a linear combination of them, amounts to pass, within Chart 1, from one expression of the CV response to another one.

Starting from the general case R + S, zones R and SR are limiting cases corresponding to the following situations. In R, diffusion of the substrate in the film is so fast that catalysis is kinetically governed solely by the catalytic reaction. The concentrations of the catalyst and of the substrate are then constant across the film as sketched in the insets of Fig. 2 for the profiles of Q form of the catalyst and A form of the substrate. Conversely in SR, the catalytic reaction is so fast that a steady state is established by mutual compensation of catalytic reaction and substrate diffusion in the film. The concentration profile of the substrate A is consequently contained in a thin reaction-diffusion layer at the film- solution boundary while the Q form of the catalyst concentration remains constant across the film.

For the following reasons, each of the three zones R + S, R and SR is subdivided into two sub-zones. They have to do with substrate diffusion from the bulk of the solution to the film/solution boundary. If the latter is rapid as compared to the rate of the catalytic reaction and/or if the scan rate is large, the substrate concentration may be viewed as constant. S-shaped current–potential curves are then expected as depicted in Fig. 3. This corresponds to the right hand part of Chart 1 and to zones R^{can}, $(R + S)^{can}$, SR^{can} in which the superscript "can" recalls the canonical S-shaped behavior.

On the opposite, when the catalytic reaction is fast and/or the scan rate low, the current limitation is rooted in substrate diffusion from the bulk of the solution to the film/solution boundary. We then reach "total catalysis" behaviors as in zones R^{tot},

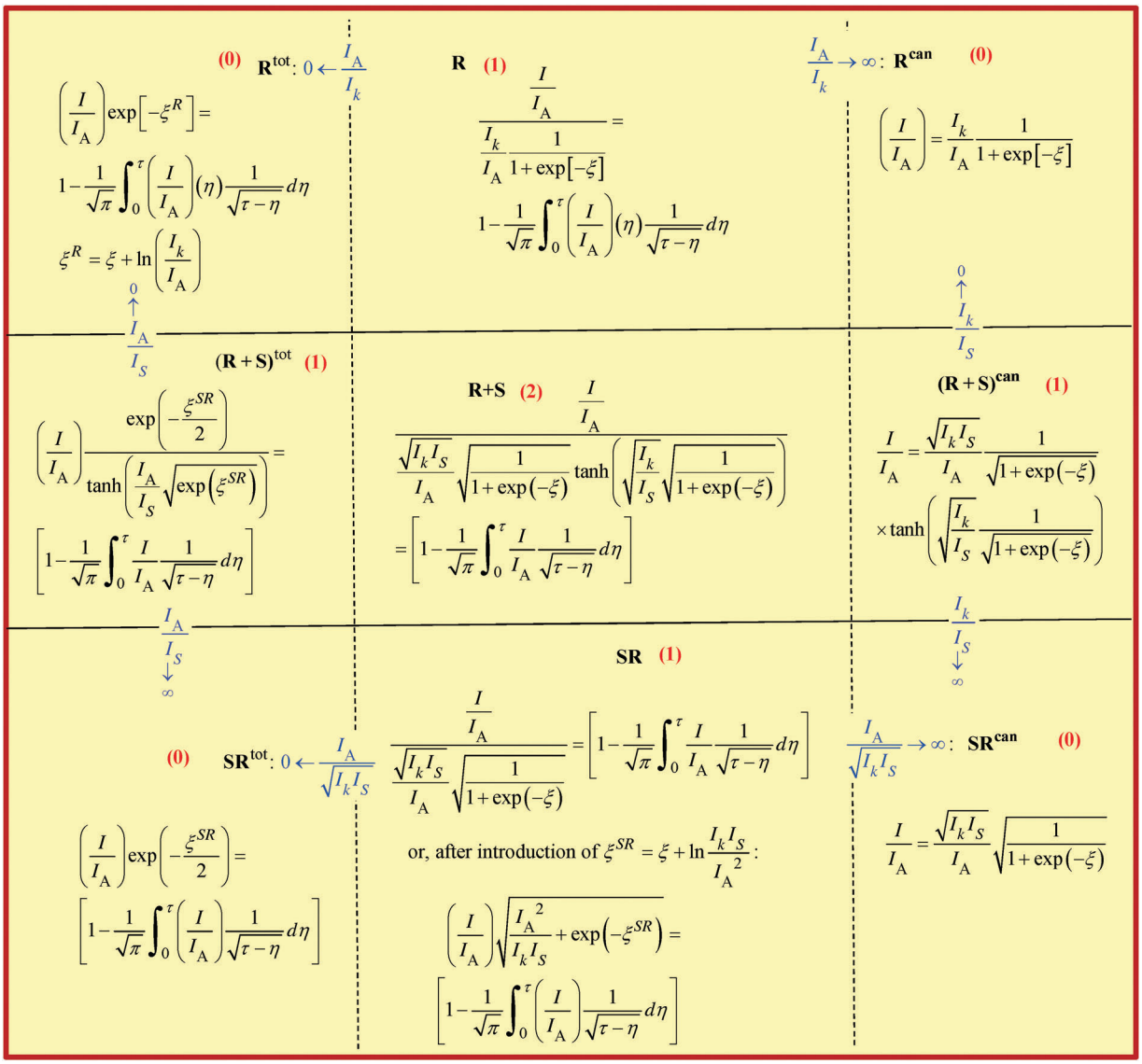

Chart 1 Current–potential responses of fast conducting films under pure kinetic conditions. In red between parentheses: number of dimensionless parameters contained in the dimension-less expressions of the CV responses as given in this chart.

$(R + S)^{tot}$, SR^{tot}. The current potential curves are then peak-shaped and largely shifted toward positive potentials (their expressions are given in the left-hand part of Chart 1 and examples are shown in Fig. 3). A precise and complete description of the effect of the experimental parameters on the passage from one zone to the other is available in Fig. 2 in the form of a compass rose.

The boundaries between various zones have been obtained by maximizing the extent of the zero-parameter *versus* the one-parameter zones, and of the latter *versus* the two-parameter zone, taking into account the experimental uncertainty: 5% of peak or plateau current (criteria on the peak potential (5%) lead to the same frontiers for $R^{tot}/(R + S)^{tot}/SR^{tot}$ transition). The equations of the CV responses corresponding to each zone are summarized in Chart 1.

The main characteristics of the current–potential responses in the zero-parameter zones – peak current density, peak potential, half-peak (or plateau) potential – are summarized in Table 1.

A systematic view of the variation of the current–potential curves with the appropriate competition parameters is given in Fig. 3. Fig. 4 provides, in a more precise manner, the variations of the plateau or peak current.

Fig. 5a, b and d depicts the variations of the half-plateau or half-peak potential, in zones R, $(R + S)^{can}$ and SR where a transition between a peak-shaped and an S-shaped responses occurs whereas the variation of the peak potential is represented in Fig. 5c for the $(R + S)^{tot}$ zone, as appropriate for the passage between two peak-shaped responses. In this last case, Fig. 6 depicts the variations of the peak width accompanying the passage through the total catalysis zones, where one passes from one peak-shaped curve to another peak-shaped curve, which however exhibits a different width.

As to the variations that the operator may carry out himself, film thickness and scan rate are the most easy to change while maintaining all other parameters constant. Passages from

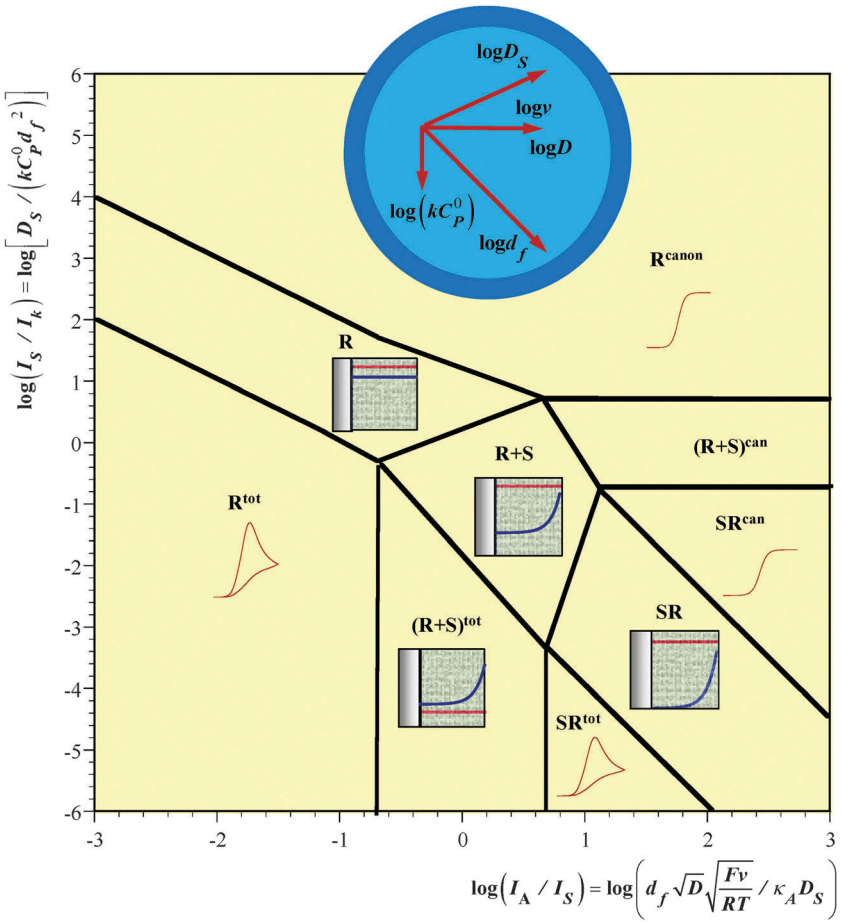

Fig. 2 Zone diagram. The insets provide schematic representations of the concentration profiles inside the film (the catalyst, Q, in red and the substrate, A, in blue). The compass rose summarized how the variations of the experimental parameters move the system from one zone to the other. The curves are only indicative of the shape of the current–potential responses. Their precise expressions are given in Chart 1. The dimensionless CV responses are shown as red curves in the zero-parameter zones.

S-shaped to a peak-shaped current–potential curve (or *vice versa*) are easy to spot. An increase of the scan rate may be used to attempt triggering the passage from a peak-shaped curve to a S-shaped curve in the crossing of the R and SR zones. A decrease of the film thickness will have the same effect in the first case and no effect in the second. We note first that S-shaped current–potential curves (zones SR^{can}, (R + S)^{can} and R^{can}) are independent of scan rate (see Fig. 2 and right hand column of Chart 1). S-shaped current–potential curves that remain S-shaped upon varying the film thickness and do not change half-wave potential indicate that the system is entrenched in the R^{can} or the SR^{can} zones. In the latter case the plateau current is independent of the film thickness, whereas it is proportional to the film thickness in the former. A decrease of the plateau current and half-wave potential with the film thickness possibly reaching saturation (Fig. 4b and 5b) would be the sign that the system is crossing the (R + S)^{can} zone. Peak-shaped current–potential curves that remain peak-shaped upon varying film thickness or scan rate with no change in the ratio peak current/square root of scan rate indicate that the system is entrenched in one of the total catalysis zones, R^{tot} or the SR^{tot}. The peak potential varies linearly in the negative direction with the log of the scan rate in both cases, by $(RT/2F)\ln 10$ (30 mV at 25 °C) in the R^{tot} zone and by $(RT/F)\ln 10$ (60 mV at 25 °C) in the SR^{tot} zone. It shifts towards negative values upon increasing the film thickness. This shift corresponds to a linear variation of E_p with $\log(d_f)$ with a slope being $(RT/F)\ln 10$ (60 mV at 25 °C) in the R^{tot} zone, whereas it is independent of the film thickness in the SR^{tot} zone. The peak width is still another criterion to distinguish the two cases: $E_{p/2} - E_p = 1.85$ and $3.80 \times (RT/F)$, for the R^{tot} or the SR^{tot} cases respectively. If, on the contrary, the peak characteristics deviate from these predictions and vary as depicted in Fig. 4c, 5c and 6 one may conclude that the system crosses the (R + S)^{tot} zone, or at least enters this zone by one or the other end.

Quantitative determination of the characteristics constants of the system

After the kinetic regime, represented by a kinetic zone or by inter-zone crossings, has been diagnosed, what are the possibilities of determining quantitatively the characteristics constants of the system?

If the situation is such that the system stands within a zero-parameter zone whatever the efforts to move it away, the following applies.

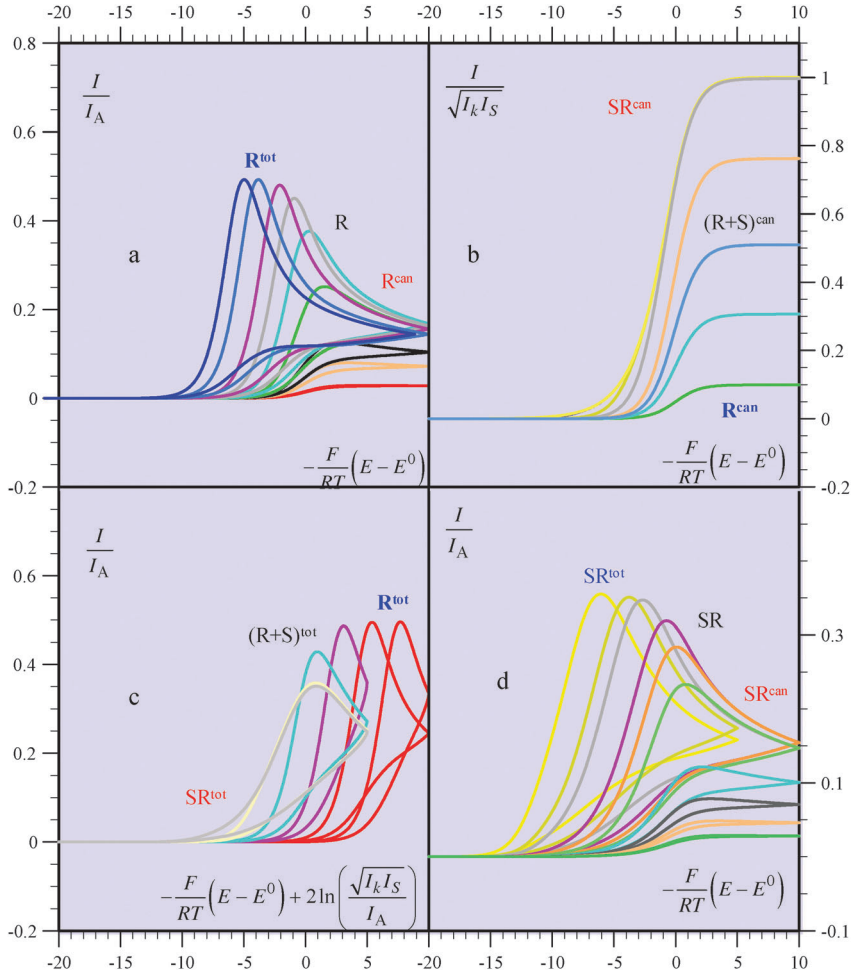

Fig. 3 Travelling through the 1-parameter zones: examples of current potential responses (a) through R, as a function of $\log\left[I_k/I_A = \left(\kappa_A k C_P^0 d_f\right)/\sqrt{DFv/(RT)}\right]$, from left to right: −2.5 (dark blue), −2 (light bue), −1.25 (magenta), −0.75 (grey), −0.25 (cyan), 0.25 (green), 0.75 (black), 1 (orange), 1.5 (red). (b) Through (R + S)^{can}, as function of $\log\left[I_k/I_S = d_f{}^2 k C_P^0/D_S\right]$, from top to bottom: 3 (yellow), 2 (dark blue), 1 (orange), 0.5 (grey), 0 (red), −0.25 (light blue), −0.5 (cyan), −1 (green). (c) Through (R + S)^{tot}, as function of $\log\left[I_A/I_S = \left(d_f\sqrt{D}\sqrt{Fv/RT}\right)/(\kappa_A D_S)\right]$, from right to left: −3 (orange), −2 (red), −1 (magenta), 0 (cyan), 1 (yellow), 2 (grey); (d) through SR, as function of $\log\left[\sqrt{I_k I_S}/I_A = \sqrt{\kappa_A k C_P^0 \kappa_A D_S RT/(FvD)}\right]$, from right to left: −1.5 (green), −1.25 (orange), −1 (dark blue), −0.75 (cyan), 0 (green), 0.25 (orange), 0.5 (red), 0.75 (violet), 1 (dark yellow), 1.5 (yellow).

Table 1 Main characteristics of the current–potential responses in the zero-parameter zones

Zone	I_p	$E_{p/2}$	$E_{p/2} - E_p$
R^{can}	$=I_k = FkC_P^0\kappa_A C_A^0 d_f$	E^0	—
SR^{can}	$= \sqrt{I_k I_S} = C_A^0\sqrt{\kappa_A\left(kC_P^0\right)\kappa_A D_S}$	$E^0 + (RT/F)\ln 3$	—
R^{tot}	$0.496 \times FC_A^0\sqrt{DFv/RT}$	$E^0 + 1.07\frac{RT}{F} + \frac{RT}{F}\ln\left(\frac{I_k}{I_A} = d_f\frac{\kappa_A k C_P^0}{\sqrt{DFv/RT}}\right)$	$1.85\frac{RT}{F}$
S^{Rtot}	$0.351 \times FC_A^0\sqrt{DFv/RT}$	$E^0 + 2.96\frac{RT}{F} + \frac{RT}{F}\ln\left(\frac{I_k I_S}{I_A{}^2} = \frac{\kappa_A k C_P^0 \kappa_A D_S}{DFv/RT}\right)$	$3.80\frac{RT}{F}$

In the R^{can} zone, the plateau current density, $I_p = I_k = FkC_P^0\kappa_A C_A^0 d_f$, and its linear variation with the film thickness allows the determination of the product of the pseudo-first order rate constant, kC_P^0, by the partition coefficient, κ_A. The half wave potential is equal to the standard potential, E^0, which can also be obtained directly when experiments with no substrate present can be carried out.

In the SR^{can} zone, the plateau current density, $I_p = \sqrt{I_k I_S} = C_A^0\sqrt{\kappa_A\left(kC_P^0\right)\kappa_A D_S}$, is inde-pendent of film thickness. By itself it gives access only to the product of the pseudo-first order rate constant, kC_P^0, by the partition coefficient, κ_A, multiplied by the product of the substrate diffusion coefficient, D_S, by the partition coefficient, κ_A. The half-wave potential, $E_{p/2} = E^0 + (RT/F)\ln 3$ is

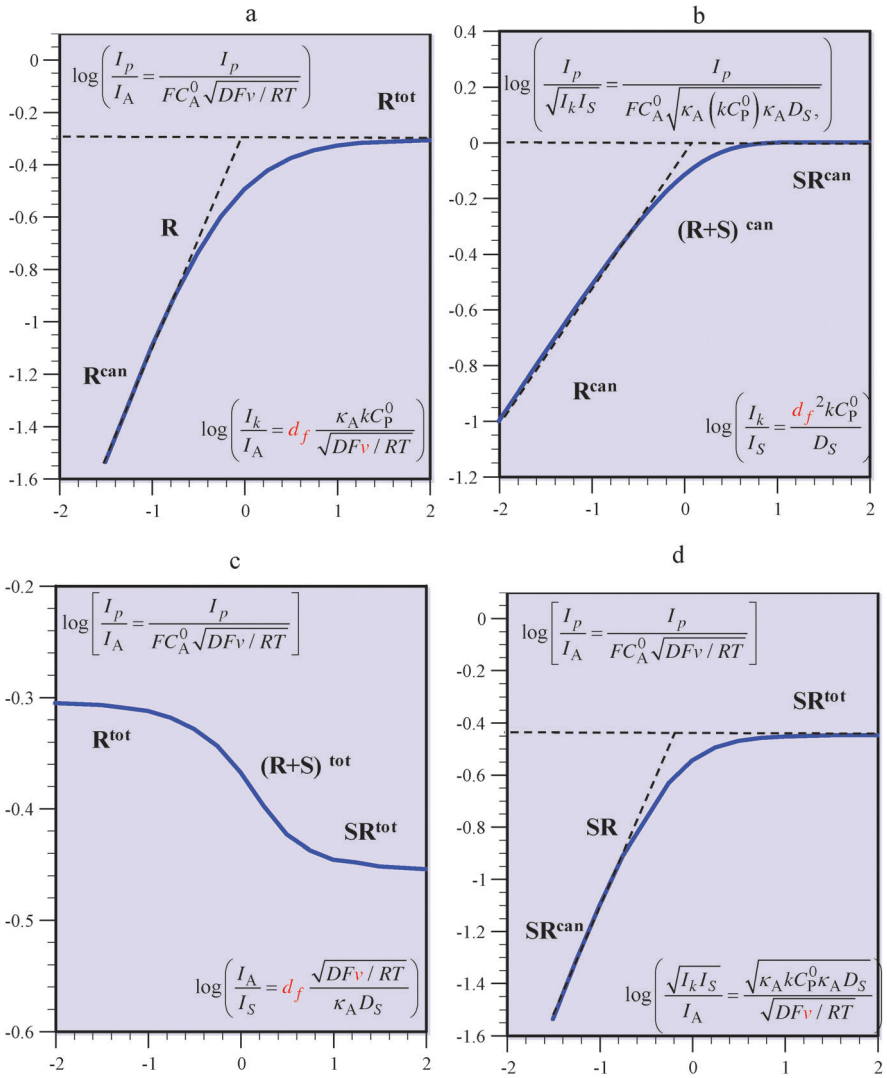

Fig. 4 Travelling through the 1-parameter zones observing the variations of the peak or plateau current.

closely related to the standard potential and does not provide new information.

In the R^{tot} zone, the peak current density, $I_p = 0.496 \times FC_A^0\sqrt{DFv/RT}$, is reflective of substrate diffusion in the solution. It does not give any information about what is going on in the film but it nevertheless provides the value of the substrate diffusion coefficient in solution, D. The kinetic information is contained in the peak potential: $E_p = E^0 - 0.78\frac{RT}{F} + \frac{RT}{F}\ln\left(\frac{I_k}{I_A}d_f = \frac{\kappa_A k C_P^0}{\sqrt{DFv/RT}}\right)$. It allows the determination of the product of the pseudo-first order rate constant, kC_P^0, by the partition coefficient, κ_A, using the above-determined value of the substrate diffusion coefficient in solution.

In the S^{tot} zone, the peak current density, $I_p = 0.351 \times FC_A^0\sqrt{DFv/RT}$, is again reflective of substrate diffusion in the solution. It does not give any information about what is going on in the film. The kinetic information is once more contained in the peak potential: $E_p = E^0 - 0.86\frac{RT}{F} + \frac{RT}{F}\ln\left(\frac{I_k I_S}{I_A{}^2} = \frac{\kappa_A k C_P{}^0 \kappa_A D_S}{DFv/RT}\right)$, which does not depends on film thickness. It gives only access to the product of the pseudo-first order rate constant, kC_P^0, by the partition coefficient, κ_A, multiplied by the product of the substrate diffusion coefficient, D_S, by the partition coefficient, κ_A.

It is worth noting that the kinetic information derived from peak potential variations in the "total catalysis" situation is the same as that obtained from plateau currents in the "canonical" situation.

We now discuss the possibilities offered by shifting the system from a zero-parameter zone to a one-parameter zone upon changing the film thickness and the scan rate.

In the "canonical situation", if the system stands initially in the R^{can} zone, a quantitative kinetic characterization of the catalytic reaction under the form of $\kappa_A kC_P^0$ is obtained. Entering the $(R + S)^{can}$ zone by means of an increase of film thickness, allows the additional determination of $\kappa_A D_S$ from the variations of the plateau current or of the half-wave potential. The situation is less simple if the system stands in the SR^{can} zone. It is then necessary to push it toward the $(R + S)^{can}$ zone if separating

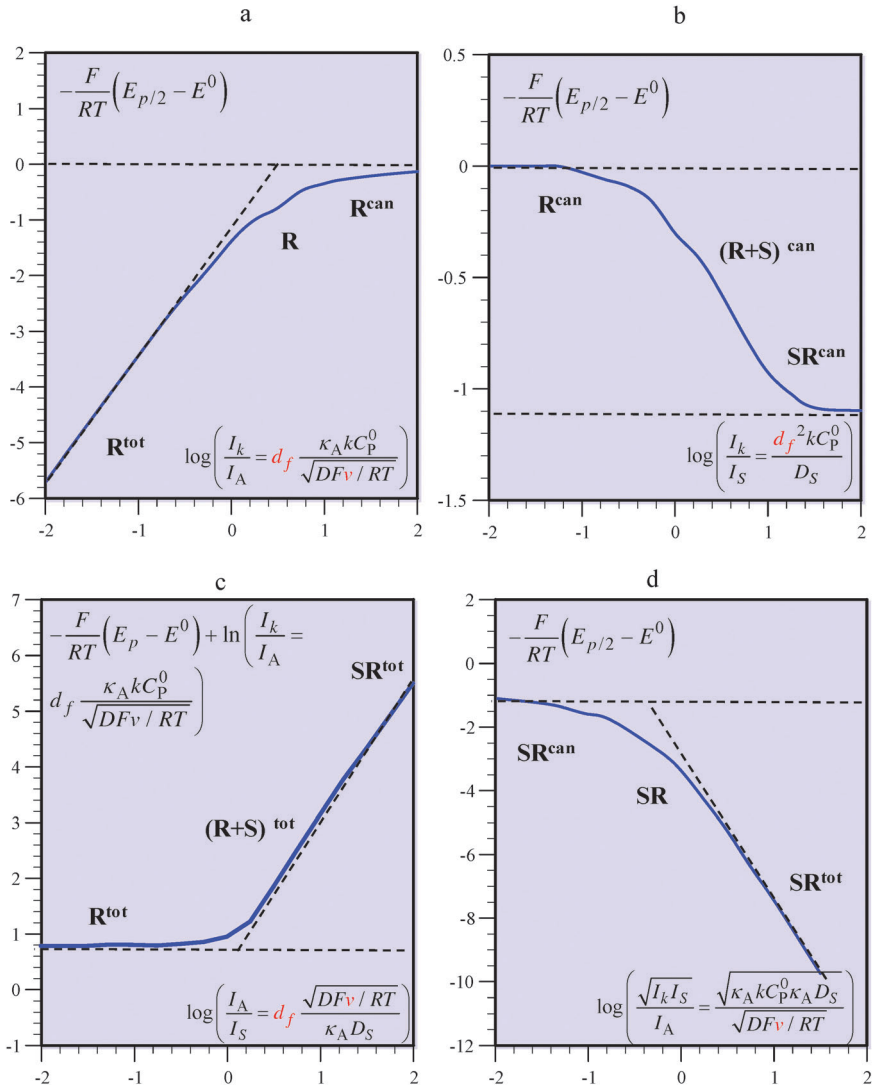

Fig. 5 Travelling through the 1-parameter zones observing the variations of the peak (E_p) or half-peak or half-wave ($E_{p/2}$) potential.

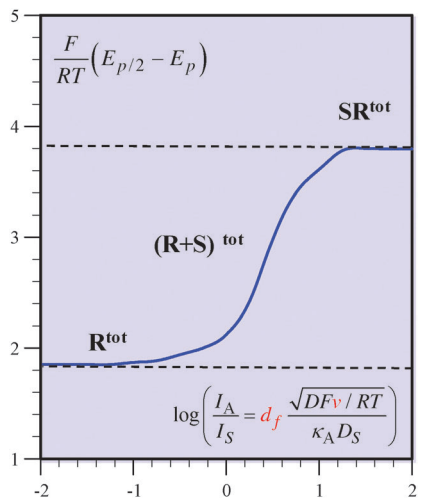

Fig. 6 Travelling through the 1-parameter total catalysis zone observing the peak width (difference between half-peak and peak potentials).

$\kappa_A kC_P^0$ from $\kappa_A D_S$ from peak current or half-wave potential variations is looked for.

In the $(R + S)^{tot}$ case, the peak potentials are, as mentioned previously, the only source of kinetic information. The best initial situation is when the system stands in the R^{tot} zone. $\kappa_A kC_P^0$ is then obtained from the variation of the half-wave potential with the film thickness. Pushing the system to the $(R + S)^{tot}$ zone by increasing the film thickness would allow the additional determination of $\kappa_A D_S$ from the variations of the half-wave potential. If the system stands initially in the SR^{tot} zone, it is mandatory to push it toward the $(R + S)^{tot}$ zone by decreasing the film thickness to obtain a separate estimation of $\kappa_A kC_P^0$ and $\kappa_A D_S$.

Increasing the scan rate may allow the passage from a peak-shaped response to an S-shaped response and *vice versa* upon crossing the R zone or the (R + S) zone or the SR zone. It is advantageous to push the system either toward a total catalysis situation or toward a canonical situation by manipulating the scan rate and then resort to the above analyses in order to gather as much kinetic information as possible.

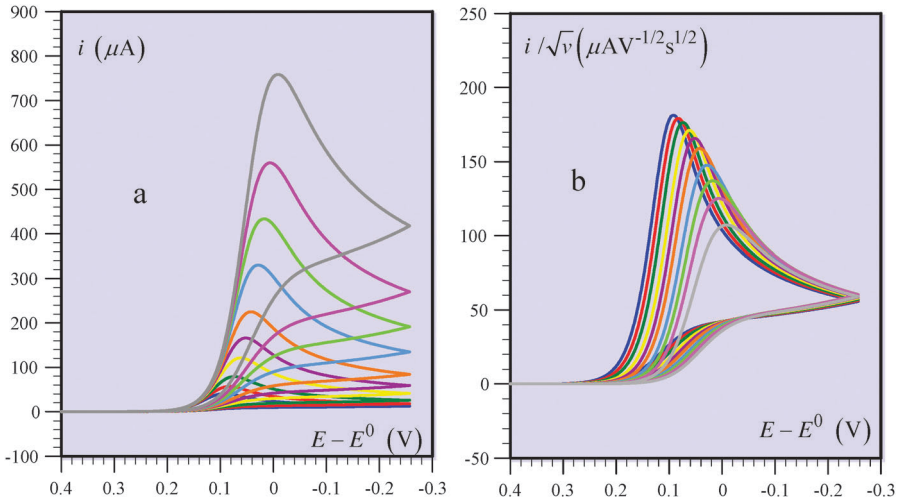

Fig. 7 Cyclic voltammetry of the system defined in the text for a film thickness d_f = 1 μm as a function of the scan rate: from bottom to top 0.05 (blue), 0.1 (red), 0.2 (green), 0.5 (yellow), 1 (magenta), 2 (orange), 5 (cyan), 10 (light green), 20 (violet), 30 (grey) V s^{-1}. (a) Raw data. (b) After division by the square root of the scan rate.

How do the preceding analyses apply when the solvent is the substrate, as *e.g.*, in catalysis of water oxidation? It suffices to consider that substrate diffusion has become infinitely rapid both in the film and in the solution. The zone diagram is simply reduced to zone R^{can}. With fast catalytic reactions, the plateau current is too large to be practically accessible and the only parameter that one can determine from the foot of the catalytic wave is $E^0 + (RT/F)\ln[\kappa_A(kC_P^0)]$. One has to be able to get out of the pure kinetic conditions, to obtain a separate estimation of E^0 and $\kappa_A(kC_P^0)$ as discussed in a preceding contribution.[9] We may note that the rate constant of the catalytic reaction has been expressed throughout the manuscript under the pseudo-order form, kC_P^0, which is indeed a pertinent parameter in the case where C_P^0 is not obtainable from experiments carried out in the absence of substrate. In all other cases discussed previously where C_P^0 can be obtained from such experiments are possible the pseudo – first order constant can immediately be converted into the second order rate constant.

A series of thought experiments

The following example illustrates how the above analyses of fast conducting electrocatalytic films can be performed in practice. The film is assumed to contain an average concentration C_P^0 = 0.05 M of active catalytic sites. Its thickness, d_f, is varied from hundreds of nanometers to tens of micrometers. In absence of substrate, a reversible surface wave[20] is observed allowing the determination the catalyst standard potential E^0 and checking the value of C_P^0. The film is coated onto a 3 mm diameter electrode (surface area S = 0.07 cm^2). Ohmic drop is minimized by means of positive feedback compensation down to a 10 Ω remaining uncompensated resistance. Consequently, if the ohmic drop is aimed to be less than 5 mV, the current has to

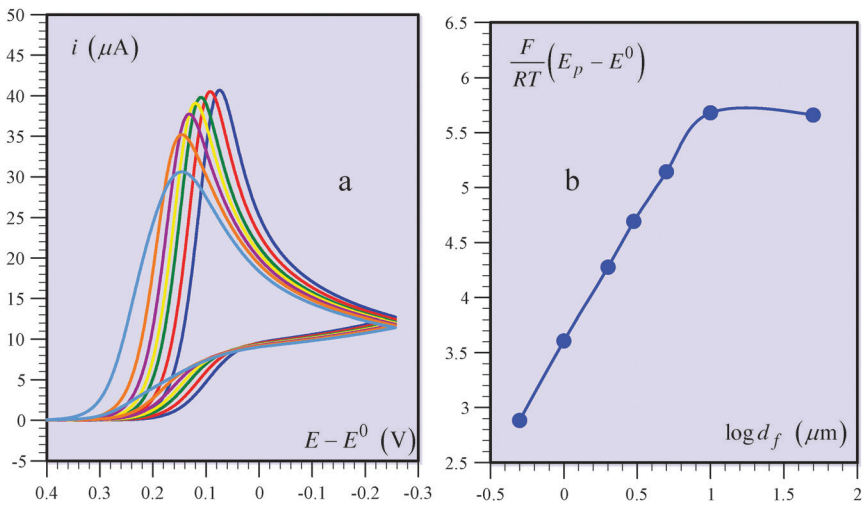

Fig. 8 Cyclic voltammetry of the system defined in the text for a scan rate of 0.05 V s^{-1} as a function of film thickness film thickness: from left to right d_f = 0.5 (light blue), 1 (orange), 2 (magenta), 3 (yellow), 5 (green), 10 (red), 50 (blue) μm. (a) Raw data. (b) Variation of the peak potential with film thickness.

be less than 500 μA (corresponding to a 7.15 mA cm^{-2} current density). This factor is expected to limit the use of high scan rate unless a concomitant decrease of the electrode diameter is envisaged. We analyze the catalytic wave obtained in the presence of a substrate concentration in solution $C_A^0 = 2 \times 10^{-3}$ M (a case where the substrate concentration is very high, as when the solvent is the substrate has been treated at the end of a preceding contributions[9]). The following strategy may be devised to extract two parameters characterizing the catalytic film, namely $k\kappa_A$ and $D_S\kappa_A$ as well as the substrate solution diffusion coefficient D. Fig. 7 and 8 show the current–potential curves obtained at several scan rates and several values of the film thicknesses. The voltammograms are peak shaped indicating that the system is far from the canonical zones. We may thus try to reach the total catalysis zones at the lowest end of the scan rate range. That this is indeed the case is attested by the almost invariance of $i_p/\sqrt{v}$ (i_p is the peak current) and by the value of the peak width, $F(E_{p/2} - E_p)/RT = 1.85$ (Fig. 7). Thus from the current–potential curve recorded at 0.05 V s^{-1}, the substrate solution diffusion coefficient D (2×10^{-5} cm^2 s^{-1}) is determined from the peak current $i_p = 0.496 \times FSC_A^0\sqrt{D}\sqrt{Fv/RT}$ and $\kappa_A k$ (10^5 M^{-1} s^{-1}) is obtained from the peak potential. The effect of film thickness, shown in Fig. 8, provides additional pieces of information. The peak potential at the lowest scan rate −0.05 V s^{-1} – *i.e.*, under total catalysis conditions, is at first a linear function of the log of film thickness which then plateaus off at a saturation value of: $E_p = E^0 - 0.86\frac{RT}{F} + \frac{RT}{F}\ln\left[k\kappa_A C_P^0 \kappa_A (D_S/D)(RT/Fv)\right]$, from which $\kappa_A D_S = 5\ 10^{-6}$ cm^2 s^{-1}.

Another strategy could have been attempted, consisting in raising the scan rate sufficiently to reach S-shaped current–potential responses. Plateau currents of 2000 μA would have been reached in the SR^{can} zone, value that is much too large to fulfill the ohmic drop limitations previously required.

Conclusion

Catalytic films in which charge propagation involves ohmic conduction are an important family of systems, particularly with the addition of various forms of carbon aimed at boosting the conductivity. Conduction is then so rapid that it limits the kinetics of the film, which is dependent on the rate of the catalytic reaction and the diffusion of the substrate inside and outside the film. In this framework, practically interesting systems are those in which catalysis is sufficiently fast for pure kinetic conditions to be fulfilled. Two opposite kinetic modes then emerge: one in which consumption of the catalyst remains negligible during the time of the cyclic voltammetric experiment giving rise to S-shaped current–potential responses (“canonical” behavior) and the other in which the current is controlled by substrate diffusion in solution (“total catalysis” behavior). Kinetic information then derives from the plateau current and its variations with film thickness in the first limiting situation and from the peak potential and its variations with the same parameters in the second case. Analysis of the system by means of a kinetic zone diagram allowed the derivation of the current–potential expressions in the various zone forming the base of a precise description of the interplay between the three kinetic-controlling factors and of the estimation of their values.

Symbols and definitions

A	Substrate
P, Q	Oxidized and reduce forms of the catalyst
C_A^0	Bulk substrate concentration
C_P^0	Total concentration of catalyst in the film
D	Diffusion coefficient of the substrate in the solution
D_S	Diffusion coefficient of the substrate in the film
E	Electrode potential
E^0	Standard potential of the catalyst couple
E_p	Peak potential
$E_{p/2}$	Half-peak or half wave potential
I	Current density
I_A	Current density characterizing substrate diffusion in the solution
I_k	Current density characterizing the catalytic reaction in the film
I_p	Peak or plateau current density
I_S	Current density characterizing substrate diffusion in the film
d_f	Thickness of the film
k	Rate constant of the catalytic reaction
t	Time
ν	Scan rate
κ_A	Partition coefficient of the substrate between solution and film
τ	Normalized time
ξ	Normalized potential

$$\tau = \frac{Fvt}{RT},\ \xi = -\frac{F}{RT}\left(E - E^0\right)$$

$$I_A = FC_A^0\sqrt{D}\sqrt{\frac{Fv}{RT}}$$

$$I_k = Fk C_P^0 \kappa_A C_A^0 d_f$$

$$I_S = F\kappa_A C_A^0 \frac{D_S}{d_f}$$

Acknowledgements

Partial support from the Agence Nationale de la Recherche (ANR CATMEC 14-CE05-0014-01) is acknowledged.

References

1 M. I. Hoffert, K. Caldeira, A. K. Jain, E. F. Haites, L. D. D. Harvey, S. D. Potter, M. E. Schlesinger, S. H. Schneider, R. G. Watts and T. M. L. Wigley, *et al.*, *Nature*, 1998, **395**, 881–884.
2 N. S. Lewis and D. G. Nocera, *Proc. Natl. Acad. Sci. U. S. A.*, 2006, **103**, 15729–15735.
3 E. E. Benson, C. P. Kubiak, A. J. Sathrum and J. M. Smieja, *Chem. Soc. Rev.*, 2009, **38**, 89–99.

4 H. B. Gray, *Nat. Chem.*, 2009, **1**, 7.
5 D. G. Nocera, *Inorg. Chem.*, 2009, **48**, 10001–10017.
6 D. Abbott, *Proc. IEEE*, 2010, **98**, 42–66.
7 S. Chu and A. Majumdar, *Nature*, 2012, **488**, 294–303.
8 V. Artero and M. Fontecave, *Chem. Soc. Rev.*, 2013, **42**, 2338–2356.
9 C. Costentin and J.-M. Savéant, *J. Phys. Chem. C*, 2015, **119**, 12174–12182.
10 H. Vrubel, T. Moehl, M. Gratzel and X. Hu, *Chem. Commun.*, 2013, **49**, 8985–8987.
11 U. A. Paulus, T. J. Schmidt, H. A. Gasteiger and R. J. Behm, *J. Electroanal. Chem.*, 2001, **495**, 134–145.
12 K. J. J. Mayrhofer, D. Strmcnik, B. B. Blizanac, V. Stamenkovic, M. Arenz and N. M. Markovic, *Electrochim. Acta*, 2008, **53**, 3181–3188.
13 M. Zhiani, H. A. Gasteiger, M. Piana and S. Catanorchi, *Int. J. Hydrogen Energy*, 2011, **36**, 5110–5116.
14 F. Jaouen, E. Proietti, M. Lefevre, R. Chenitz, J.-P. Dodelet, G. Wu, H. T. Chung, C. M. Johnston and P. Zelenay, *Energy Environ. Sci.*, 2011, **4**, 114–130.
15 A. Le Goff, V. Artero, B. Jousselme, P. D. Tran, N. Guillet, R. Metaye, A. Fihri, S. Palacin and M. Fontecave, *Science*, 2009, **326**, 1384–1387.
16 X. Zhu, J. B. Kerr, Q. He, G. Hwang, Z. Martin, K. Clark, A. Z. Weber and N. Zhao, *ECS Trans.*, 2012, **45**, 143–152.
17 C. P. Andrieux and J.-M. Savéant, *Molecular Design of Electrode Surfaces*, ed. R. W. Murray, John Wiley and Sons, New York, NY, 1992, vol. 22, p. 207.
18 J.-M. Savéant, *Elements of molecular and biomolecular electrochemistry: an electrochemical approach to electron transfer chemistry*, John Wiley & Sons, Hoboken, NJ, 2006, pp. 268–297.
19 J.-M. Savéant, *Elements of molecular and biomolecular electrochemistry: an electrochemical approach to electron transfer chemistry*, John Wiley & Sons, Hoboken, NJ, 2006, vol. 82, pp. 106–119.
20 J.-M. Savéant, *Elements of molecular and biomolecular electrochemistry: an electrochemical approach to electron transfer chemistry*, John Wiley & Sons, Hoboken, NJ, 2006, pp. 2–5.